

SUPPORTING INFORMATION

Preparation of a Semiquinonate-Bridged Diiron(II) Complex and Elucidation of its Geometric and Electronic Structures

Amanda E. Baum, Sergey V. Lindeman and Adam T. Fiedler*

EXPERIMENTAL SECTION

General methods: All reagents and solvents were purchased from commercial sources and used as received unless otherwise noted. Dichloromethane was purified and dried using a Vacuum Atmospheres solvent purification system. The compounds 2,5-dimethoxyhydroquinone¹ and $K(\text{Ph}_2\text{Tp})^2$ were prepared according to literature procedures. The synthesis of complex **1** was reported in our previous manuscript.³ The synthesis and handling of air-sensitive materials were carried out under an inert atmosphere using a Vacuum Atmospheres Omni-Lab glovebox.

Preparation of [2]PF₆: $[\text{Fe}_2(\text{Ph}_2\text{Tp})_2(\mu\text{-DMHQ})]$ (**1**, 98.0 mg, 0.0605 mmol) was treated with one equivalent of AgPF_6 (16.1 mg, 0.0637 mmol) in CH_2Cl_2 (10 mL) for one hour. The resulting dark brown solution was filtered through celite and concentrated to approximately half of its original volume. Layering of this solution with pentane provided dark brown needles suitable for X-ray crystallography (69 mg, 62%). The X-ray structure found one uncoordinated CH_2Cl_2 molecule per unit cell, and elemental analysis indicates that some solvent (~0.4 equiv.) remains after drying. Anal. Calcd for $\text{C}_{98}\text{H}_{76}\text{B}_2\text{F}_6\text{Fe}_2\text{N}_{12}\text{O}_4\text{P}\cdot 0.4\text{CH}_2\text{Cl}_2$ (MW = 1797.99 g mol^{-1}): C, 65.73; H, 4.31; N, 9.35. Found: C, 65.77; H, 4.00; N, 9.54. FTIR (cm^{-1} , solid): 3051, 2616 [$\nu(\text{B-H})$], 1516, 1495, 1477, 1464, 1431, 1414, 1207, 1163, 1065, 1009, 833, 759, 694, 668.

Physical measurements: Elemental analyses were performed at Midwest Microlab, LLC in Indianapolis, IN. Infrared (IR) spectra of solid samples were measured with a Thermo Scientific Nicolet iS5 FTIR spectrometer equipped with the iD3 attenuated total reflectance accessory. UV-vis spectra were obtained with an Agilent 8453 diode array spectrometer. Magnetic susceptibility measurements were carried out using the Evans NMR method.

Cyclic voltammetric (CV) measurements were conducted in the glovebox with an epsilon EC potentiostat (iBAS) at a scan rate of 100 mV/s with 100 mM (NBu₄)PF₆. A three-electrode cell containing a Ag/AgCl reference electrode, a platinum auxiliary electrode, and a glassy carbon working electrode was employed. Under these conditions, the ferrocene/ferrocenium (Fc⁺⁰) couple has an E_{1/2} value of +0.52 V in CH₂Cl₂.

EPR experiments were performed using a Bruker ELEXSYS E600 equipped with an ER4415DM cavity resonating at 9.63 GHz, an Oxford Instruments ITC503 temperature controller and ESR-900 He flow cryostat. The program EasySpin⁴ was used to simulate the experimental spectra.

Resonance Raman (rR) spectra were obtained upon excitation with a Coherent I-305 Ar⁺ laser with ~45 mW of laser power at the sample. The scattered light was collected using a 135° backscattering arrangement, dispersed by an Acton Research triple monochromator equipped with a 1200 grooves/mm grating and analyzed with a Princeton Instruments Spec X 100BR deep depletion, back-thinned CCD camera. Solution samples of **1** and [**2**]PF₆ were prepared in CD₂Cl₂ with concentrations of 4.8 and 3.1 mM, respectively. Spectra were accumulated at 77 K by inserting the samples (contained in an NMR tube) in an EPR dewar filled with liquid N₂. rR excitation profiles were measured by quantifying the sample peak intensities relative to the 1032 cm⁻¹ peak of frozen CD₂Cl₂.

Crystallographic studies: X-ray diffraction (XRD) data were collected with an Oxford Diffraction SuperNova kappa-diffractometer (Agilent Technologies) equipped with dual microfocus Cu/Mo X-ray sources, X-ray mirror optics, Atlas CCD detector, and low-temperature Cryojet device. The data were processed with CrysAlis Pro program package (Agilent Technologies, 2011) typically using a numerical Gaussian absorption correction (based on the real shape of the crystal), followed by an empirical multi-scan correction using SCALE3 ABSPACK routine. The structures were solved using SHELXS program and refined with SHELXL program⁵ within Olex2 crystallographic package.⁶ B- and C-bonded hydrogen atoms were positioned geometrically and refined using appropriate geometric restrictions on the corresponding bond lengths and bond angles within a riding/rotating model (torsion angles of methyl hydrogens were optimized to better fit the residual electron density).

Crystallographic data for [2]PF₆•CH₂Cl₂: C₉₉H₇₈B₂Cl₂F₆Fe₂N₁₂O₄P, $M_r = 1848.95 \text{ g mol}^{-1}$, triclinic, space group *P*-1, $a = 9.7382(3)$, $b = 13.2530(4)$, $c = 18.0619(7) \text{ Å}$, $\alpha = 103.453(3)$, $\beta = 104.559(3)$, $\gamma = 97.098(3)^\circ$, $V = 2152.89(13) \text{ Å}^3$, $Z = 1$, $\rho = 1.428 \text{ g cm}^{-3}$, total data 42432, independent reflections 8566 ($R_{\text{int}} = 0.0395$), 624 parameters, $R_1 = 0.0393$ for $I \geq 2\sigma(I)$ and $wR_2 = 0.1024$.

DFT calculations: DFT calculations were performed using the ORCA 2.8 software package developed by Dr. F. Neese.⁷ Geometry optimizations employed the Becke-Perdew (BP86) functional,⁸ while single-point (SP) and time-dependent DFT (TD-DFT) calculations used Becke's three-parameter hybrid functional for exchange along with the Lee-Yang-Parr correlation functional (B3LYP).⁹ SP and TD-DFT calculations were based on modified crystallographic coordinates in which the phenyl groups at the 5-position of the pyrazole ligands were replaced by hydrogen atoms. Ahlrichs' valence triple- ζ basis set (TZV), in conjunction with the TZV/J auxiliary basis set,¹⁰ were used for all calculations. TD-DFT calculations¹¹ computed absorption energies and intensities within the Tamm-Dancoff approximation.¹² In each case, at least 60 excited states were calculated. The gOpenMol program¹³ developed by Laaksonen was used to generate isosurface plots of molecular orbitals.

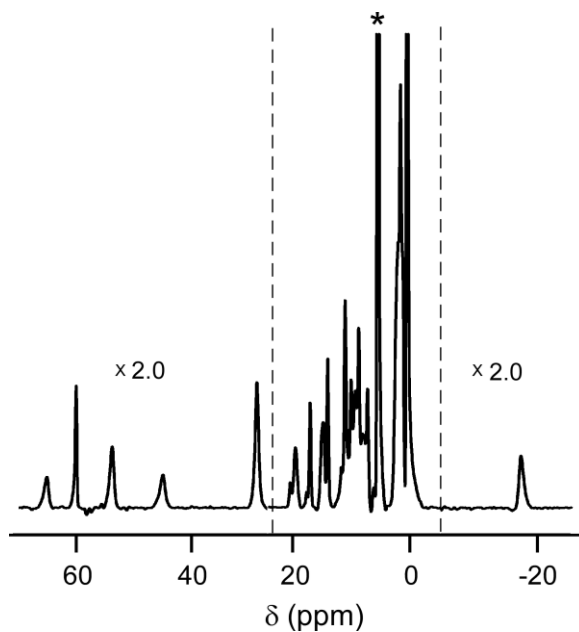


Figure S1. ^1H NMR spectra of **1** in CD_2Cl_2 . Peak intensities for the outer portions of the spectra were enlarged ($\times 2$) for the sake of clarity. The solvent-derived peak is indicated with an asterisk(*).

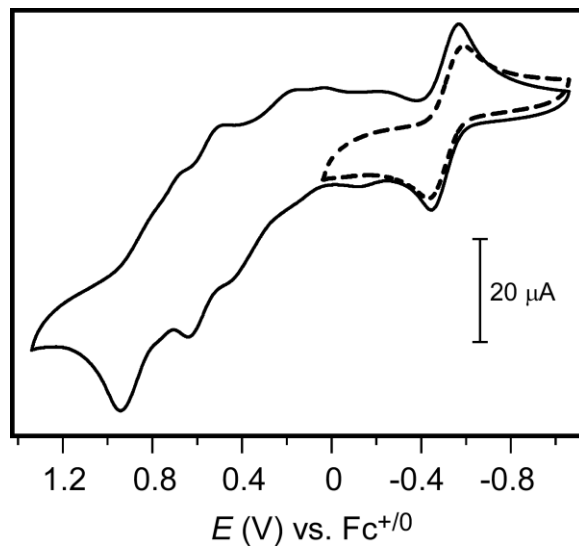


Figure S2. Cyclic voltammograms of complex **1** measured in CH_2Cl_2 with 100 mM $(\text{NBu}_4)\text{PF}_6$ as the supporting electrolyte and a scan rate of 100 mVs^{-1} .

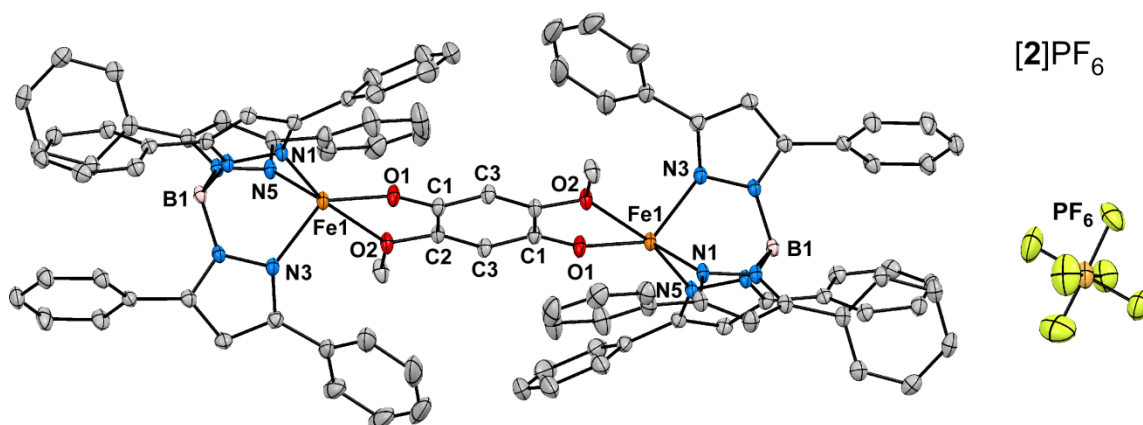


Figure S3. Thermal ellipsoid plot (50% probability) derived from the X-ray structure of $[2]PF_6 \cdot CH_2Cl_2$. Non-coordinating solvent molecules and hydrogen atoms have been omitted for clarity. Key metric parameters are provided in Table 1.

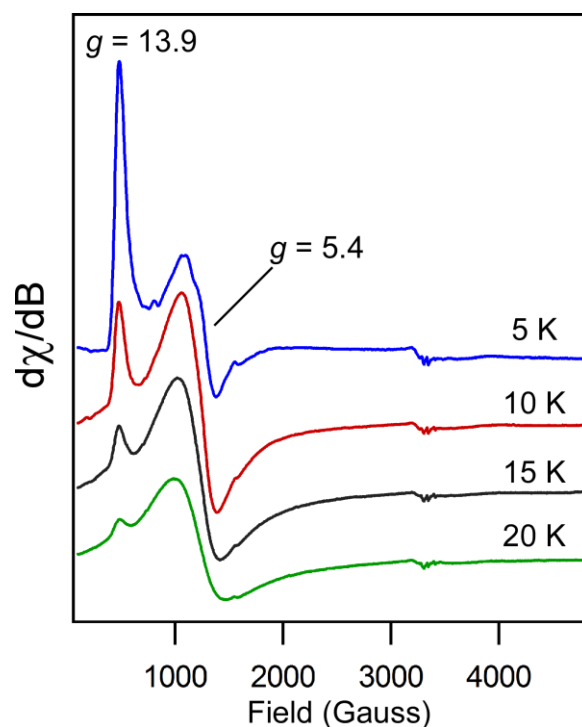


Figure S4. X-band EPR spectra of $[2]PF_6$ at various temperatures (5, 10, 15, and 20 K) in frozen CH_2Cl_2 solution (4 mM). Experimental parameters: frequency = 9.38 GHz; microwave power = 2.0 mW; modulation amplitude = 10.0 Gauss; modulation frequency = 100 kHz.

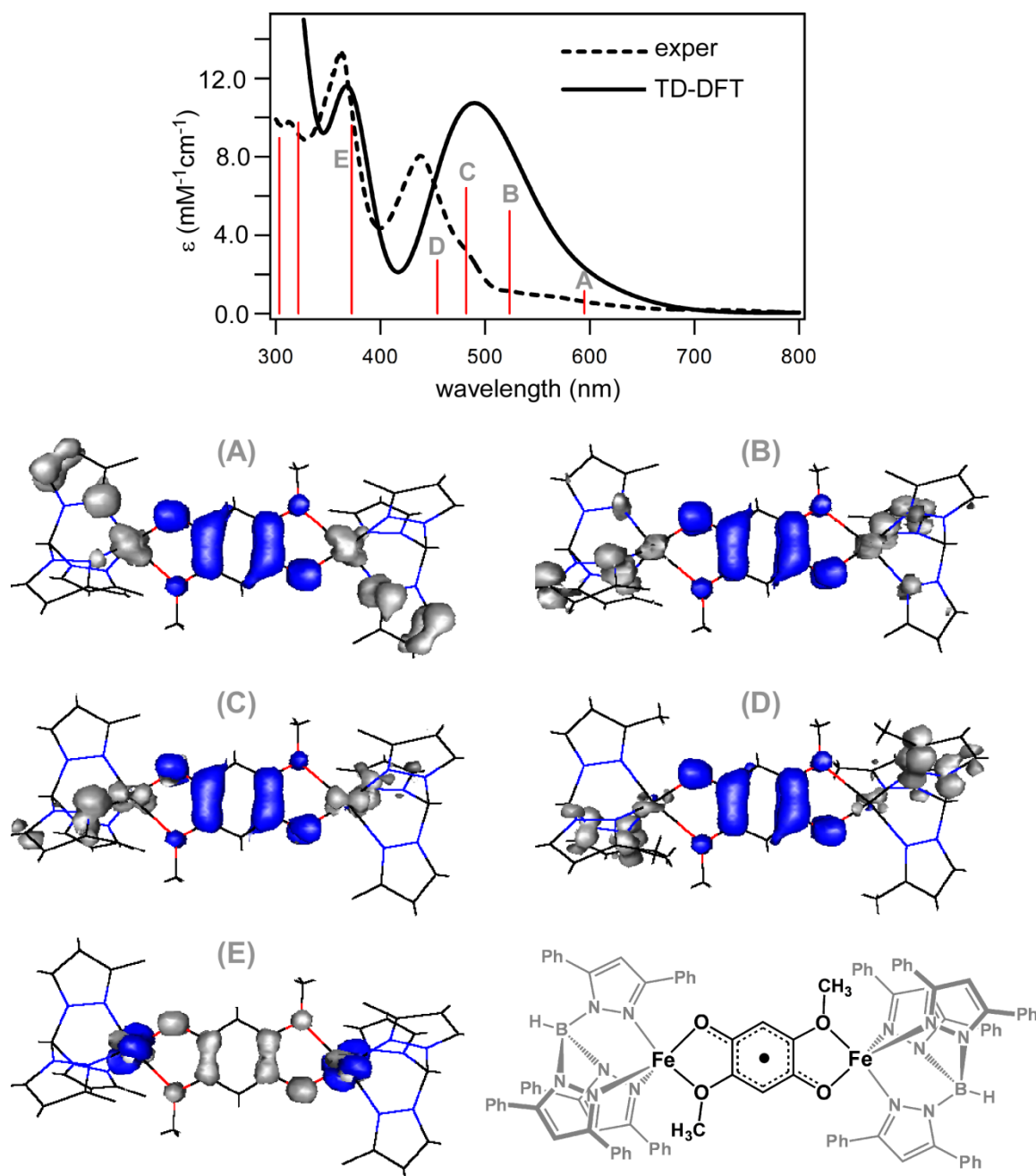


Figure S5. Top: Experimental (dashed) and TD-DFT computed (solid line) absorption spectra for $[\mathbf{2}]\text{PF}_6$. Red sticks represent the energies and intensities of prominent transitions in the TD-DFT spectrum. Bottom: Electron density difference maps (EDDMs) for the computed transitions labeled in the upper spectrum. Blue and grey regions indicate gain and loss of electron density, respectively.

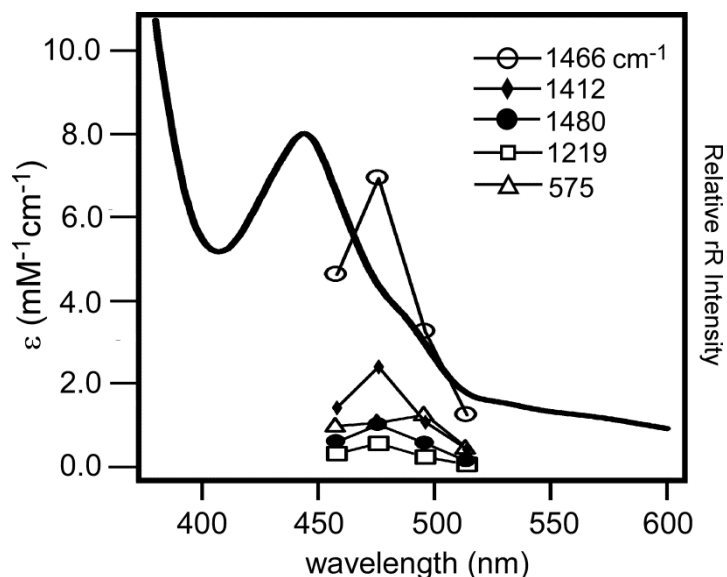


Figure S6. rR excitation profiles of various modes of [2]PF₆ measured with a frozen CD₂Cl₂ solution ([Fe] = 3.1 mM) at 77 K. Profiles are superimposed on the room temperature absorption spectrum of [2]PF₆ in CH₂Cl₂.

References

1. D. Hanss, M. E. Walther and O. S. Wenger, *Chem. Commun.*, 2010, **46**, 7034-7036.
2. N. Kitajima, K. Fujisawa, C. Fujimoto, Y. Morooka, S. Hashimoto, T. Kitagawa, K. Toriumi, K. Tatsumi and A. Nakamura, *J. Am. Chem. Soc.*, 1992, **114**, 1277-1291.
3. A. E. Baum, H. Park, D. N. Wang, S. V. Lindeman and A. T. Fiedler, *Dalton Trans.*, 2012, **41**, 12244-12253.
4. S. Stoll and A. Schweiger, *Journal of Magnetic Resonance*, 2006, **178**, 42-55.
5. G. M. Sheldrick, *Acta Crystallogr. Sect. A*, 2008, **64**, 112-122.
6. O. V. Dolomanov, L. J. Bourhis, R. J. Gildea, J. A. K. Howard and H. Puschmann, *J. Appl. Crystallogr.*, 2009, **42**, 339-341.
7. F. Neese.
8. (a) A. D. Becke, *J. Chem. Phys.*, 1986, **84**, 4524-4529; (b) J. P. Perdew, *Physical Review B*, 1986, **33**, 8822-8824.
9. (a) A. D. Becke, *J. Chem. Phys.*, 1993, **98**, 5648-5652; (b) C. T. Lee, W. T. Yang and R. G. Parr, *Physical Review B*, 1988, **37**, 785-789.

10. (a) A. Schafer, H. Horn and R. Ahlrichs, *J. Chem. Phys.*, 1992, **97**, 2571-2577; (b) A. Schafer, C. Huber and R. Ahlrichs, *J. Chem. Phys.*, 1994, **100**, 5829-5835.
11. (a) R. E. Stratmann, G. E. Scuseria and M. J. Frisch, *J. Chem. Phys.*, 1998, **109**, 8218-8224; (b) M. E. Casida, C. Jamorski, K. C. Casida and D. R. Salahub, *J. Chem. Phys.*, 1998, **108**, 4439-4449; (c) R. Bauernschmitt and R. Ahlrichs, *Chem. Phys. Lett.*, 1996, **256**, 454-464.
12. (a) S. Hirata and M. Head-Gordon, *Chem. Phys. Lett.*, 1999, **314**, 291-299; (b) S. Hirata and M. Head-Gordon, *Chem. Phys. Lett.*, 1999, **302**, 375-382.
13. L. Laaksonen, *J. Mol. Graph.*, 1992, **10**, 33-&.